Articles

STM and TS Study of InAs Quantum Dots Immobilized on Au and Pt Surfaces

Lara I. Halaoui,[†] Richard L. Wells,[‡] and Louis A. Coury, Jr.*[,‡]

Department of Chemistry, American University of Beirut, Beirut, Lebanon 110236, and Department of Chemistry, P. M. Gross Chemical Laboratory, Duke University, Durham, North Carolina, 27708

Received May 13, 1999. Revised Manuscript Received February 17, 2000

The first study of the electrical properties of nanometer-size InAs particles is presented. InAs quantum dots (Q-InAs) deposited as films onto Pt and Au electrodes are examined using scanning tunneling microscopy (STM), tunneling spectroscopy (TS), and macroscopic conductivity measurements. In addition, single Q-InAs particles adsorbed on Au-covered mica substrates are examined by STM. The following results are reported in this study: (1) The size distribution of Q-InAs obtained from cross sections of STM images agreed with previous XRD and TEM size measurements, and the measured size was well below the exciton diameter estimated for InAs. (2) The TS $I-V$ curves for Q-InAs films on Au show a larger zero-current region than that obtained for sulfide-passivated, bulk single crystal *p*-InAs; consistent with the magnitude of strong confinement predicted for particles of this size by the effective mass model. (3) Macroscopic $I-V$ measurements acquired under vacuum for Q-InAs films deposited onto Au interdigitated array electrodes show the absence of an effect of charge transport at either the Q-InAs/Q-InAs or the Q-InAs/Au interfaces on TS energy gap measurements. These results supported our conclusion that the zero-current region in the TS spectra of Q-InAs is reflective of a wider HOMO−LUMO gap in the quantum dots. These $I-V$ plots also showed that the conductivity of the Q-films is only 2 orders of magnitude lower than bulk InAs.

Introduction

Research on semiconductors of nanometer dimensions is motivated by the unique properties that quantum-confined (or Q-) semiconductors are expected to exhibit, and by a variety of potential applications (viz., nonlinear optical devices, optoelectronics, solar cells).[1] Nanomaterials research has included investigations of quasi-two-dimensional (quantum well) and quasi-one-dimensional (quantum wire) materials.[2] The technological advances achieved so far through the use of multilayered quantum heterostructures (e.g., high efficiency lasers)[3] have led to an increased interest in studying structures of even lower dimensionality in search of more pronounced confinement effects.

In quasi-zero-dimensional materials or quantum dots (QD), electrons are spatially confined along all three directions.[1b,d] This confining potential will result in a fully quantized eigenspectrum with the QD behaving as a superatom, exhibiting discrete, atomic-like energy levels.[4] The extent of quantization will primarily depend on the number of atoms constituting the dot as well as on its shape.[4] In Q-semiconductors, in particular, quantum confinement effects cause the energy gap region to become larger than the bulk band gap (E_g). This effect is expected to be observed when the size of the nanoparticle is comparable to a critical length scale, suggested by Brus to be the 1S-exciton diameter.[5] Members of the III−V family of semiconductors are expected to exhibit quite pronounced quantum confinement effects, at a relatively large size scale, because of the small effective masses of the hole and electron and the large dielectric constant of these materials, which give rise to large exciton diameters relative to the II−VI family.

* Corresponding author. Current address: Bioanalytical Systems, Inc., 2701 Kent Ave., West Lafayette, IN 47906. e-mail: coury@bioanalytical.com.

[†] American University of Beirut.

[‡] Duke University.

(1) (a) Stucky, G. D.; McDougall, J. E. *Science* **1990**, *247*, 669. (b) Brus, L. E.; Steigerwald, M. L. *Acc. Chem. Res.* **1990**, *23*, 183. (c) Stucky, G. D. *Prog. Inorg. Chem.* **1992**, *40*, 99. (d) Weller, H. *Adv. Mater.* **1993**, *5*, 88. (e) Siegel, R. W. *Phys. Today* **1993**, *46(10)*, 64.

(2) Miller, R. J. D.; McLendon, G. L.; Nozik, A. J.; Schmickler, W.; Willig, F. In *Surface Electron-Transfer Processes*; VCH Publishers: New York, 1995; Chapter 6 and references therein.

(3) (a) Burnham, R. D.; Streifer, W.; Paoli, T. L. *J. Cryst. Growth* **1984**, *68*, 370. (b) Tsang, W. T. In *Semiconductors and Semimetals*; Willardson, R. K., Beer, A. C., Eds.; Academic Press: New York, 1987; Vol. 24, p 397.

(4) Grundmann, M.; Christen, J.; Ledentsov, N. N.; Böhrer, J.; Bimberg, D.; Ruvimov, S. S.; Werner, P.; Richter, U.; Gösele, U.; Heydenreich, J.; Ustinov, V. M.; Egorov, A. Yu.; Zhukov, A. E.; Kop'ev, P. S.; Alferov, Zh. I. *Phys. Rev. Lett.* **1995**, *74*, 4043.

(5) Brus, L. E. *J. Chem. Phys.* **1984**, 80, 4403.

10.1021/cm9902927 CCC: $19.00
Published on Web 04/06/2000

InAs is a narrow band gap III−V semiconductor (E_g = 0.36 eV at 300 K for bulk material), whose energy gap can be tuned from the near infrared to the visible region, depending on the extent of quantization.[6]

Experimental investigations of QDs are hampered by the difficulties associated with making measurements on a single QD. The information thus obtained may differ from that obtained from arrays of particles, for which measured properties will be averaged over the whole ensemble. Grundmann et al.[4] have been able to observe very narrow cathodoluminescence lines arising from single Q-InAs dots in a GaAs matrix, showing for the first time the presence of an atomic-like δ-functional density of states, a quantum confinement effect long predicted for Q-semiconductors.[4] In addition, InAs nanocrystals between 1 and 8 nm in size have been shown to exhibit a significant third-order optical nonlinearity.[6] However, aside from reports of observed blueshifts in absorption edges for suspensions of Q-semiconductors, including Q-InAs prepared using a modification of the dehalosilylation reaction used in this work,[6,7] and our initial results using tunneling spectroscopy to probe the energy gap in Q-InAs films,[8] no other band gap measurements have been reported for III−V semiconductor QDs.

Scanning tunneling spectroscopy (STS), or tunneling spectroscopy (TS), has been used to determine the density of states within the band gap region, as well as band gap widths and positions of band edges for semiconductors. Both current−voltage (I vs V) and conductivity measurements (dI/dV vs V) have been reported.[9−17] Results have been published for several materials including Si,[9] GaAs,[10] n-TiO_2,[11] InAs/GaSb superlattices,[12] and CdS[13] and CdSe[14] QDs. STS has also proved useful in combination with an optical probe in studying the electrooptical properties of bulk semiconductors[18] and quantum well structures (e.g., $InAs_xP_{1-x}$/InP).[19] Because of the small size of the STM tip, TS has the potential of probing the electronic properties of one or a few QDs at a time.

In this paper, we discuss STM, TS, and conductivity measurements of chemically synthesized Q-InAs.[20] STM images of Q-InAs films and single particles deposited on metal surfaces are reported, and reveal dimensions well below the estimated exciton diameter for InAs. TS is used to probe the energy gap region of Q-InAs and of bulk InAs passivated with a sulfide layer, and reveal a wider energy gap for the QDs relative to the bulk solid; consistent with the magnitude of strong quantum confinement predicted for particles of this size. Current−voltage measurements under vacuum of Q-InAs films on Au interdigitated array electrodes are also reported. Results show the absence of an effect of charge conduction at the particle/particle and particle/metal interfaces on energy gap measurement of Q-InAs from the tunneling spectra zero-current region. We also report a room temperature conductivity for Q-InAs films only 2 orders of magnitude lower than the bulk solid.

Experimental Section

Materials. Q-InAs samples were prepared using a synthetic route described in detail elsewhere.[20] Briefly, this method involves a dehalosilylation reaction between an indium trihalide and $As(SiMe_3)_3$ and was found to yield nanocrystallites of purity as high as 99.96% after thermal annealing.[20c] The average domain size was determined to be 9 nm from the X-ray diffraction (XRD) peak broadening, using the Debye−Scherrer equation.[20c] Q-InAs was stored in an argon-filled Dri-Lab HE-243 (Vacuum Atmospheres) to protect the surface against air oxidation.[21] Single-crystal, Zn-doped, p-type InAs wafers (Atomet, Inc.) with a 4×10^{18} cm^{-3} carrier concentration and a (100) $\pm$ 0.5° crystal orientation were used.

Metallic Contact to Wafers. Ohmic contact to the backside of the *p*-InAs wafers was established by evaporating 1550 Å of Au (Alfa-ÆSAR) over 150 Å of Zn (Alfa-ÆSAR). Before metal deposition, the wafers were etched for 30 s with H_2O/H_3PO_4/H_2O_2 (25:3:1 by volume), followed by 30 s in 1:1 HCl/H_2O, rinsed with deionized (DI) water (resistivity $\geq$ 18.1 MΩ cm), then dried under a dry nitrogen flow. $I-V$ plots of the resulting back contact were measured using a 4145A semiconductor parameter analyzer (Hewlett-Packard), and showed ohmic behavior with a contact resistance of 6.5−7.5 Ω, obtained without thermal annealing.

Passivation of Single-Crystal p-InAs. Samples of *p*-InAs 0.5−1.0 cm in length were etched prior to use in 2% Br_2 in methanol for 10 s, then in 6 M HCl for 3 s, followed by rinsing with DI water. For studies on unpassivated surfaces, the wafers were dried in an Ar stream and stored under vacuum. For sulfide passivation studies, the freshly etched wafers were immediately immersed for 5 min in 0.5 M sodium sulfide aqueous solution ($Na_2S{\cdot}9H_2O$, Aldrich) in DI water,[22] rinsed with DI water, dried, and stored in vacuo.

Metal Substrates. Planar, polycrystalline Pt and Au (AAI-AbTech) were used as substrates onto which the films were adsorbed. These substrates consisted of a sputter coating of Au or Pt (1000 Å) over a titanium adhesion layer (100 Å) on electronics grade borosilicate glass. Substrates of Au deposited on mica disks were used for imaging of single Q-InAs particles.

(6) Uchida, H.; Matsunaga, T.; Yoneyama, H.; Sakata, T.; Mori, H.; Sasaki, T. *Chem. Mater.* **1993**, *5*, 716.
(7) See, e.g., (a) Wang, Y.; Suna, A.; Mahler, W.; Kasowski, R. J. *J. Chem. Phys.* **1987**, *87*, 7315. (b) Miyoshi, H.; Yamachika, M.; Yoneyama, H. *J. Chem. Soc., Faraday Trans.* **1990**, *86*, 815. (c) Olshavsky, M. A.; Goldstein, A. N.; Alivisatos, A. P. *J. Am. Chem. Soc.* **1990**, *112*, 9438. (d) Mićić, O. I.; Sprague, J. R.; Curtis, C. J.; Jones, K. M.; Machol, J. L.; Nozik, A. J.; Giessen, H.; Fluegel, B.; Mohs, G.; Peyghambarian, N. *J. Phys. Chem.* **1995**, *99*, 7754. (e) Guzelian, A. A.; Banin, U.; Kadavanich, A. V.; Peng, X.; Alivisatos, A. P. *Appl. Phys. Lett.* **1996**, *69*, 1432. (f) Guzelian, A. A.; Katari, J. E. B.; Kadavanich, A. V.; Banin, U.; Hamad, K.; Juban, E.; Alivisatos, A. P.; Wolters, R. H.; Arnold, C. C.; Heath, J. R. *J. Phys. Chem.* **1996**, *100*, 7212.
(8) Halaoui, L. I.; Kher, S. S.; Lube, M. S.; Aubuchon, S. R.; Hagan, C. R.; Wells, R. L.; Coury, L. A. Jr. *ACS Symp. Ser.*; Chow, G.-M., Gonsalves, K. E., Eds. **1996**, 622, 178.
(9) Fan, F.-R. F.; Bard, A. J. *J. Phys. Chem.* **1990**, *94*, 3761.
(10) Fan, F.-R. F.; Bard, A. J. *J. Phys. Chem.* **1991**, *95*, 1969.
(11) Fan, F.-R. F.; Bard, A. J. *J. Phys. Chem.* **1993**, *97*, 1431.
(12) Feenstra, R. M.; Stroscio, J. A.; Fein, A. P. *Surf. Sci.* **1987**, *181*, 295.
(13) Ogawa, S.; Fan, F.-R. F.; Bard, A. J. *J. Phys. Chem.* **1995**, *99*, 11182.
(14) Alperson, B.; Cohen, S.; Rubinstein, I.; Hodes, G. *Phys. Rev. B* **1995**, *52*, 17017.
(15) Feenstra, R. M.; Stroscio, J. A.; Tersoff, J.; Fein, A. P. *Phys. Rev. Lett.* **1987**, *58*, 1192.
(16) Märtensson, P.; Feenstra R. M. *Phys. Rev. B* **1989**, *39*, 7744.
(17) Feenstra R. M.; Collins, D. A.; Ting, D. Z.-Y.; Wang, M. W.; McGill, T. C. *J. Vac. Sci. Technol. B* **1994**, *12*, 2592.
(18) Qian, Q. L.; Wessels, B. W. *Appl. Phys. Lett.* **1991**, *58*, 1295.
(19) Qian, Q. L.; Wessels, B. W. *Appl. Phys. Lett.* **1991**, *58*, 2538.
(20) (a) Wells, R. L.; Pitt, C. G.; McPhail, A. T.; Purdy, A. P.; Shafieezad, S.; Hallock, R. B. *Chem. Mater.* **1989**, *1*, 4. (b) Wells, R. L.; McPhail, A. T.; Purdy, A. P.; Shafieezad, S.; Hallock, R. B. *Mater. Res. Soc. Symp. Proc.* **1989**, *131*, 45. (c) Wells, R. L.; Aubuchon, S. R.; Kher, S. S.; Lube, M. S.; White, P. S. *Chem. Mater.* **1995**, *7*, 793.
(21) Bartels, F.; Mönach, W. *Vacuum* **1990**, *41*, 667 and references therein.
(22) (a) Berkovitz, V. L.; Bessolov, V. N.; L'vova, E. B.; Novikov, V. I.; Safarov, R. V.; Khasieva, R. V.; Tsarenkov, B. V. *Fiz. Tekh. Poluprovodn.* **1991**, *25*, 1406; *Sov. Phys. Semicond.* **1991**, *25*, 847. (b) Kudryavtsev, E. B.; Novikov, E. B.; Stus, N. M.; Chaikina, E. I. *Fiz. Tekh. Poluprovodn.* **1992**, *26*, 1742; *Sov. Phys. Semicond.* **1992**, *26*, 975.

A total of 1500 Å of 99.99% Au was deposited under vacuum at a rate of 0.2−0.3 nm/s onto the mica disks (Digital Instruments). The mica disks were allowed to equilibrate at 228 °C before the deposition. After depositing Au, the Au/mica substrates were annealed for an hour at 245 °C and then allowed to cool to room temperature under vacuum. Au-covered mica surfaces were shown by STM and AFM to be substantially flatter than commercial polycrystalline Au and Pt surfaces and were thus suitable for single particle imaging.

Particle Immobilization for STM and TS Studies. Q-InAs particles were suspended in ACS grade methanol (Fisher) by sonicating the mixture for 30−60 s in a Branson 1200 ultrasonic cleaning bath, to break up any aggregation in the sample. Methanol was reported to contain less than 0.02% water and was used instead of water because the oxidation of III−V semiconductors reported to occur in some aqueous systems has not been similarly noted in methanol.[23] In addition, in a previous study on Q-GaAs particles by Wells et. al, methanol was shown to chemically cap these particles and thus results in a better suspension. To form Q-InAs films, 10−20 drops from a Pasteur pipet of a 0.4−0.6 mg/mL suspension were deposited onto the Au or Pt substrates (coverage area = 0.4 cm^2) and warmed gently to evaporate the methanol. Using the above amounts and coverage area, film thicknesses can be calculated to be 0.5−0.9 μm, by assuming a uniform distribution of the particles on the surface. Before complete evaporation of methanol, the Q-InAs films were admitted to a vacuum chamber (for subsequent TS measurements). The use of methanol as a suspension medium, evaporation at low temperature (<40 °C), and the subsequent complete drying under vacuum were the steps taken to minimize the oxidation of these III−V semiconductor particles upon exposure to air or water. For single particle imaging, less than 4 drops of Q-InAs/methanol dilute suspension were deposited onto the Au-on-mica substrate and methanol was evaporated under ambient conditions.

Sulfide Passivation of Q-InAs. Q-InAs stored under Ar was added to 0.5 M Na_2S in deoxygenated, deionized (DODI) water for 2 min. The solution was deoxygenated by bubbling Ar for 20 min. (Use of DODI water is reported to prevent the growth of surface oxide layers on III−V materials such as GaAs.[24]) The solution was then centrifuged (Becton Dickinson Compact II centrifuge; 3200 rpm); the particles were collected, washed with DI water, and suspended in methanol.

TS under Nonconductive Fluid. TS measurements were performed under silicone oil (dimethyl silicone; CAS registry no. 63148−62−9; Thomas Scientific) as the bathing fluid. A drop of the oil was deposited on the sample in situ underneath the tip before engaging the approach mechanism. Conductive carbon tape (SPI, West Chester, PA) was used to establish electrical contact between the STM stage and the metal substrate. The sample stage was at ambient temperature and pressure, and was covered by a solid metal Faraday cage, thus shielding samples from light.

STM Tips. Pt/Ir tips (Nanotips; Digital Instruments) or electrochemically etched W tips were used for acquisition of data. STM images were obtained with both types of tips, while TS data were collected only with Pt/Ir tips. To form W tips, W wires (Aldrich) of 0.25 mm diameter were electrochemically etched in 5% sodium nitrite solution (Aldrich) using a 30 V (peak-to-peak) ac voltage. The tips were then rinsed with DI water and coated with WD-40 to prevent oxidation.[25] Only sharp Pt/Ir tips were used to acquire the STM images, while Pt/Ir tips which were blunt were used in collecting some of the TS data.[11]

Apparatus. STM and TS data were acquired in air or under fluid using a Nanoscope II or a Nanoscope III STM (Digital Instruments, Inc). A scan rate of 19.5 Hz was used in the STM imaging of films, while a 5.09 Hz scan rate was used in the STM imaging of single particles. To obtain TS data, local $I-V$ plots were acquired at a fixed tip−sample separation using the Nanoscope software. Each TS spectrum shown represents a single, internally averaged $I-V$ plot (average count = 40). The energy gap measurements reported represent mean values calculated from a number of different $I-V$ spectra obtained at one location on a given sample (Q-InAs film or passivated wafer). Conductance plots (dI/dV vs V) were obtained by differentiating the original TS current−voltage data.

Current−Voltage Measurements of Q-InAs Films on Au IDA Electrodes. Macroscopic $I-V$ data for Q-InAs films deposited on Au interdigitated array (IDA) electrodes were collected by cyclic voltammetry (CV) using a microprocessor-controlled potentiostat (EG&G Princeton Applied Research, model 263) and commercial software (EG&G PAR model 270). The Au IDA electrodes (AAI-AbTech) consisted of two sets of 50 parallel, interdigitated microband Au electrodes on borosilicate glass. Each microband electrode consisted of 5 μm wide by 5 mm long Au strip, separated from an opposing electrode by a 5 μm space. The protective coating on each IDA was removed in acetone, the electrodes were washed further with hexane, followed by isopropyl alcohol, and then rinsed with DI water and dried under vacuum.

The $I-V$ measurements using IDAs (referred to as macroscopic to distinguish them from TS data) were conducted in a two-electrode mode, with the applied voltage representing the potential drop between adjacent fingers on the electrode. The $I-V$ plots were collected either (1) in an Ar-filled Dri-Lab (Vacuum Atmospheres, HE−243), or (2) under a vacuum of 28−30 mm of Hg inside a Duo-Vac oven (Lab-Line Instruments) at room temperature. Electrical connections to the vacuum chamber were installed and sealed with a silicone polymer (General Electric). $I-V$ plots of the IDA electrodes were acquired prior to film deposition to ensure the absence of any surface conductivity. Films of particles were formed on Au IDAs by solvent casting using 100−350 μL volumes of a 2.5 mg/mL Q-InAs suspension in methanol. The wet films were admitted into vacuum for drying and remained under vacuum for at least 3−4 h before any electrical measurements were performed. For electrical measurements under argon, films were dried in a small vacuum chamber (held at 50 mmHg), then admitted into the argon-filled chamber.

Results and Discussion

STM Images and Particle Size Distribution. Polycrystalline Pt substrates, rinsed in methanol and dried in air, were imaged prior to particle deposition. Figure 1 shows a typical constant-height image of such a Pt surface acquired with a Pt/Ir tip, using a sample bias voltage of 80.0 mV, and a 2.0 nA set-point current. STM imaging showed the surface to be sufficiently smooth for films of Q-InAs to be distinguished above the background corrugation.

Q-InAs films deposited on Pt surface were imaged by STM using Pt/Ir and W tips. Figures 2a and 3a show 500 nm scan range of Q-InAs-on-Pt films, acquired using a Pt/Ir tip with the constant-height and constant-current modes, respectively, at a bias voltage of 100.1 mV and 1.0 nA set-point current. The same sample was imaged using a W tip (image not shown), and no significant difference in the images was observed. The above scans reveal the Q-InAs particles to be fairly uniformly distributed on the imaged surface. The STM images were not different in consecutive scans, and therefore imaging did not appear to cause disruption of the particles' interaction with the surface. No surface treatment of either Q-InAs or the Au or Pt substrates was necessary to cause the adsorption of the QDs onto

(23) (a) Barbé, H.; Van Meirhaeghe, R. L.; Cardon, F. *Semicond. Sci. Technol.* **1988**, *3*, 853. (b) Liliental-Weber, Z.; Geib, K. M.; Wilmson, C. W.; Geib, K. M.; Kirchner, P. D.; Baker, J. M.; Woodall, J. M. *J. Appl. Phys.* **1990**, *67*, 1863.

(24) Hirota, Y.; Ogino, T.; Watanabe, Y.; Oshima, M. *Appl. Phys. Lett.* **1994**, *65*, 2036.

(25) Nanoscope II & III Instrument Manuals, Digital Instruments: Santa Barbara, CA.

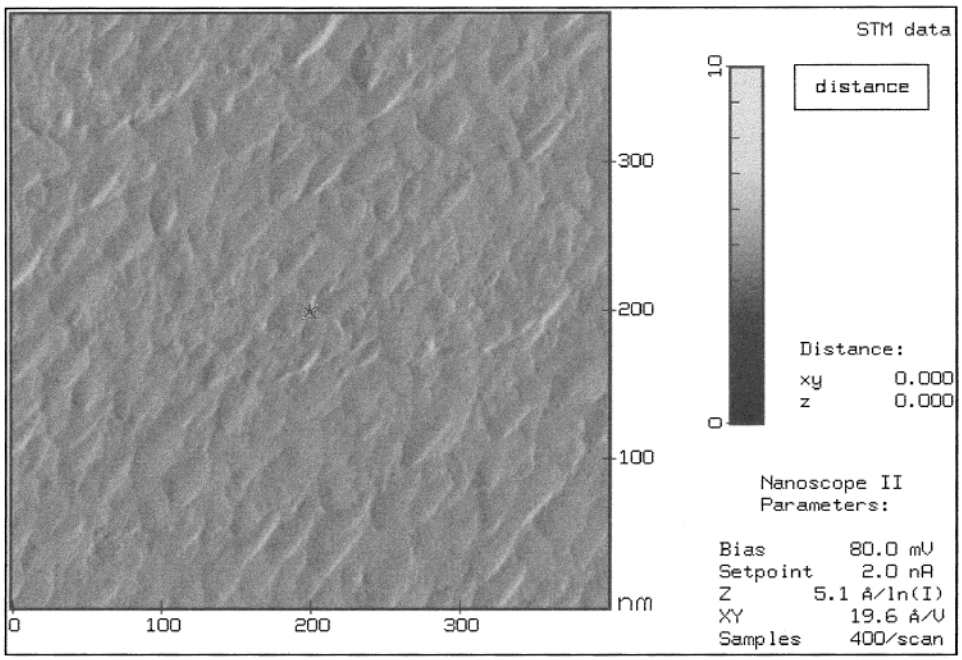

Figure 1. STM surface image of polycrystalline Pt surface prior to particle deposition, acquired with a sharp W tip at a bias voltage of 80.0 mV and 2.0 nA set-point current.

these surfaces. Similarly, GaAs has been shown to interact strongly with Au.[26] A number of semiconductor−metal interactions have been investigated by Hiraki et al.[27] who have concluded that compound semiconductors with energy gaps less than about 2.5 eV diffuse readily into various metals at room temperature; this may explain the strong Q-InAs adsorption observed in this work.

Sequential cross sections of images were taken along the *yz* plane, through particles that did not appear to be aggregates, and the size distribution was determined by measuring the particles' widths. The size determination gave mean diameter values of 11 ± 4 nm and 18 ± 6 nm from the constant-height and constant-current images, respectively (Pt/Ir tip; sample size = 120 particles for each determination). The best-fit Gaussian functions for the histograms, shown in Figures 2b and 3b, had coefficients of determination (R^2) of 0.936 and 0.953 and centroids of 10.2 and 15.6 nm, respectively. A mean diameter of 12 ± 3 nm was derived from an image obtained with a W tip in the constant-height mode. The average diameter from the *constant-height* images (11 nm) was in good agreement with the XRD-measured crystallite size (9 nm). The mean diameter (18 nm) determined from the *constant-current* image was, on the other hand, considerably larger than the XRD determined size. This could be attributed to the fact that the tip, to maintain a constant tunneling current, must partially descend into the crevices between the particles, thus causing the lateral dimension in the constant-current images to be more susceptible to tip size effects, and to become enlarged. The STM-measured size was also consistent with previous size measurements from transmission electron microscopy (TEM) data, which revealed crystallites of 8.4−22.4 nm in size.[20c]

Single Q-InAs particles deposited onto Au-covered mica surfaces (Figure 4) were also imaged by STM, both in air and under silicone fluid (under which the TS experiments are performed), and no significant difference in images was observed between the different environments. Figure 5a shows a 250 nm scan of Q-InAs on Au-on-mica acquired in air with a Pt/Ir tip using the constant-current mode, at a bias voltage of 200 mV, and a 1.0 nA set-point current. Figure 5b is a 70 nm scan, showing the region in Figure 5a containing the particles. A number of single particles can be clearly distinguished in the 70 nm scan, with the feature in the center showing an aggregate of two or more particles. The particles shown have diameters ranging from 10 to 18 nm. Since the QDs' geometry is expected to affect their properties, we report an aspect ratio for ellipsoidal particles ranging between 1.3 and 1.7 from STM and AFM imaging (not shown).

The horizontal dimension of the investigated samples was larger than the apparent height in the constant-current images (the constant-height mode does not provide topographic information in the *z* direction). In the constant-current STM image of Q-InAs films (Figure 3a), for instance, nonaggregated particles with 20 nm diameter exhibited *z* dimensions of ∼4 nm. From the lateral resolution in these images (∼2−4 nm), and by assuming the tip−sample separation distance to be 1−2 nm, which is a typical value for a conducting surface at the specified bias voltage and set-point current,[28a] the tip radius can be estimated to be 44 nm using the approximation that the lateral resolution is [2 Å (R + s)]$^{1/2}$.[28b] (R is the tip radius and s is the tip−sample separation distance). In this case, the tip radius is comparable to the particle size, and STM images will

(26) (a) Weiser, V. G.; Fatemi, N. S. *J. Appl. Phys.* **1988**, *64*, 4618. (b) Hagan, C. R. S.; Kher, S. S.; Halaoui, L. I.; Wells, R. L.; Coury, L. A., Jr. *Anal. Chem.* **1995**, *67*, 528.

(27) Hiraki, A.; Kim, S.; Kammura, W.; Iwami, M. *Surf. Sci.* **1979**, *86*, 706.

(28) (a) Elings, V.; Wiedman, J. *Am. Lab.* **1989**, *21*, 34. (b) Tersoff. J.; Hammann. D. R. *Phys. Rev. Lett.* **1983**, *50*, 1998; **1985**, *B32*, 805.

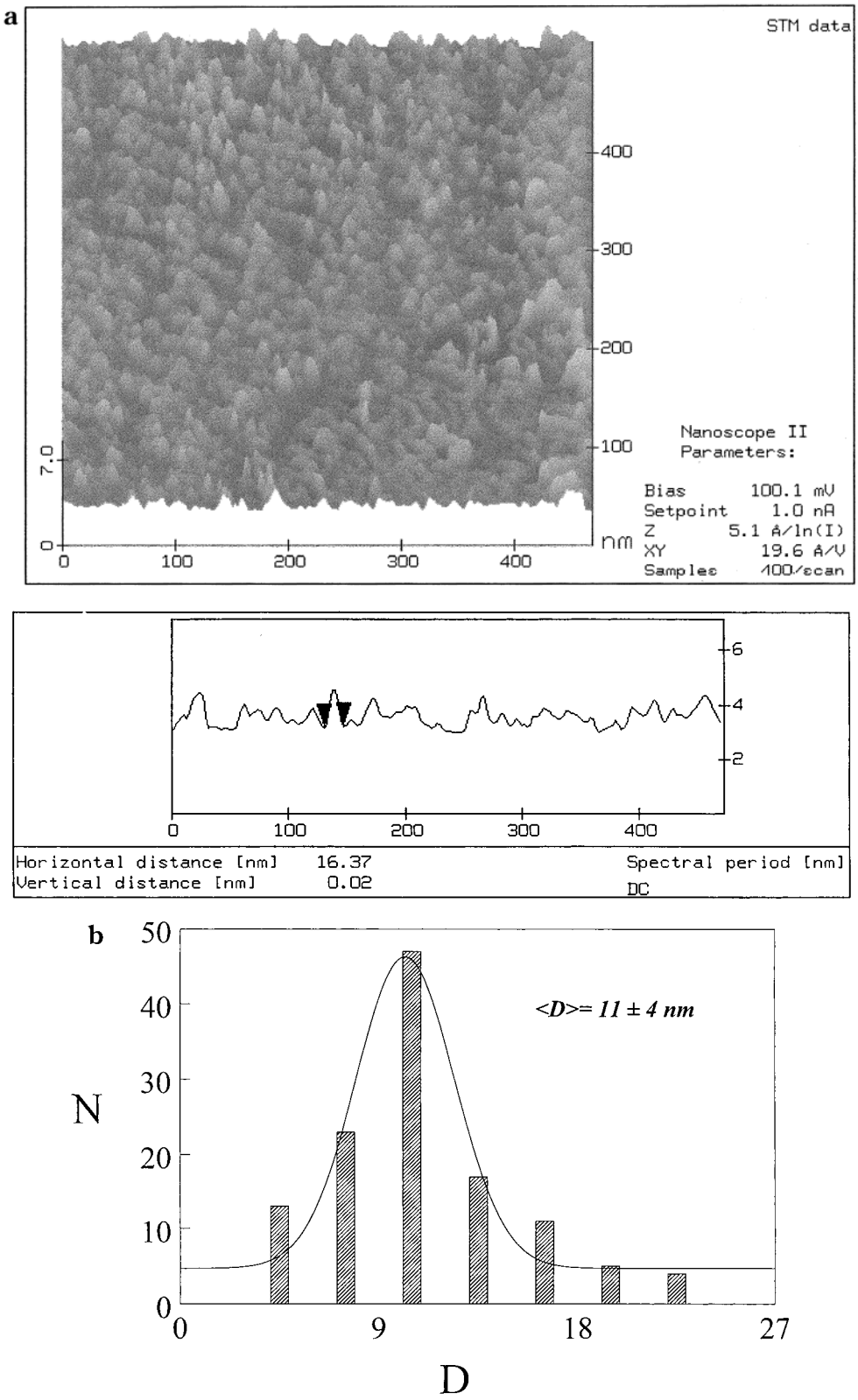

Figure 2. Constant-height STM image of Q-InAs deposited on Pt, with a Pt/Ir tip at a bias voltage of 100 mV and 1.0 nA current (a), and the size distribution with the best-fit Gaussian function (b).

be a convolution of the imaged particles and the tip. The tip will not be able to penetrate in the spaces between closely spaced particles in the constant-current mode, thus causing the vertical dimension to be strongly dependent on the tip size and shape, and to be suppressed accordingly.[29,30] On the other hand, the horizontal dimension will be relatively only slightly en-

(29) Gimsewski, J. K.; Humbert, A.; Bednorz, J. G.; Reihl, B. *Phys. Rev. Lett.* **1985**, *55*, 951.
(30) Reiss, G.; Vancea, H.; Wittmann, J.; Zweck, J.; Hoffman, H. *J. Appl. Phys.* **1990**, *67*, 1156.

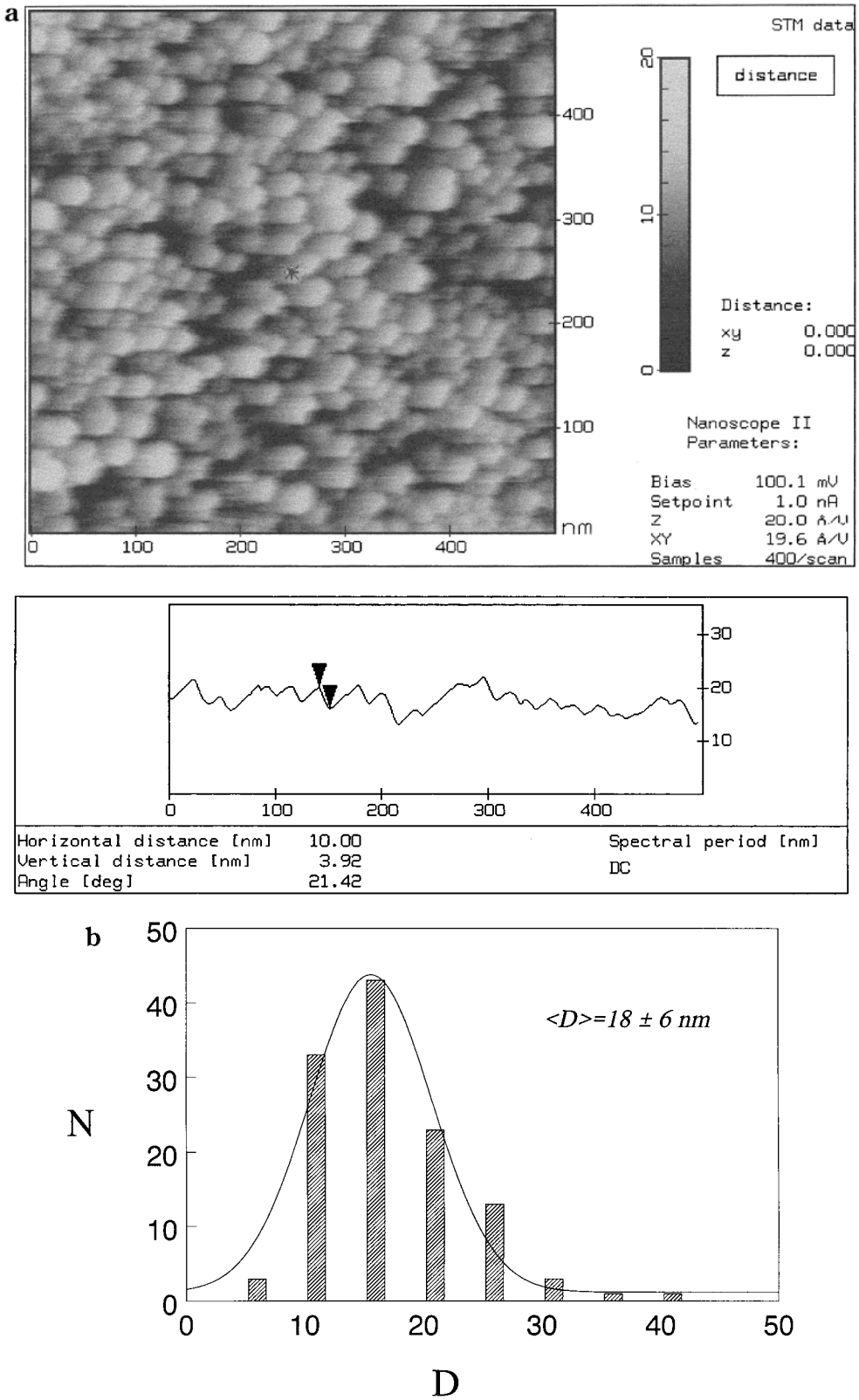

Figure 3. Constant-current STM image of Q-InAs deposited on Pt with a Pt/Ir tip at a bias voltage of 100 mV and 1.0 nA current (a), and the size distribution with the best fit Gaussian function (b).

larged, and can be reproduced with sufficient accuracy using different tips.[29,30] Deconvoluting the image to obtain height measurements is not feasible in this case, even when imaging single Q-InAs on Au, for the following reason. In addition to its dependence on distance, the tunneling current also depends on differences in the density of electronic states between Q-InAs dots and the nearby metal substrate (case of single particle imaging), and between different size Q-InAs particles (case of Q-InAs films). A Q-InAs cluster with a low density of states will appear shorter than it is when imaged placed on a metal surface, for instance. In fact, height measurements of seven out of eight particles examined in STM images of single particles

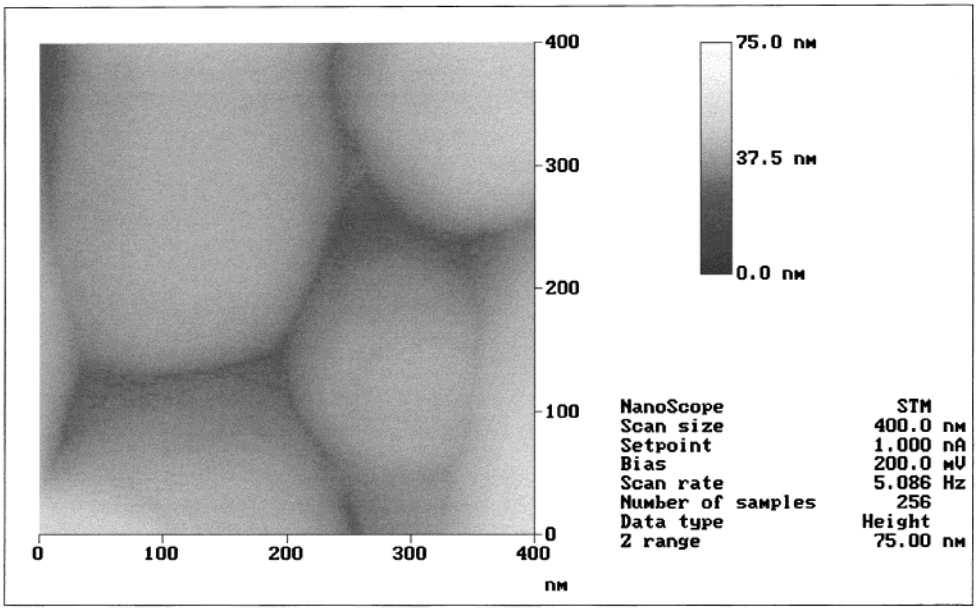

Figure 4. Constant-current STM image of Au-on-mica substrate acquired with a Pt/Ir tip at a 200 mV bias voltage and 1.0 nA set-point current.

on Au ranged between 2 and 6 nm; the eighth exhibited a height of 10 nm. More accurate height measurements were obtained from AFM images (not shown), which revealed a height of 8−10 nm for 5 out of 12 particles examined (42%), consistent with STM and XRD results.

TS Studies for Q-InAs and Bulk p-InAs. The Bohr radius (a_B) for InAs can be calculated using the following equation for compound semiconductors:[31]

$$a_B = \hbar^2 \frac{4\pi\epsilon_r\epsilon_o}{e^2}\left(\frac{1}{m_e{}^* m_e} + \frac{1}{m_h{}^* m_e}\right)$$

where m_e is the electron free mass, $m_e{}^*$ (0.0219) and $m_h{}^*$ (0.35) are the effective masses for the electron and hole in InAs respectively,[32] e is the fundamental charge, ϵ_r is the high-frequency dielectric constant for bulk InAs (12.25),[32] and ϵ_o is the permittivity of vacuum. According to this calculation, particles with diameters comparable to 62.8 nm (twice the Bohr radius of 31.4 nm) should exhibit quantum confinement effects. The onset of confinement effects for III−V semiconductors occurs at considerably larger dimensions relative to II−VI Q-particles such as CdS, whose exciton diameter is about 6 nm.[5] The Q-InAs clusters examined in this work have mean particle diameters at least *seven standard deviation units* below the dimension of 62.8 nm.

The most widely sought confinement effect is the increase in the energy gap predicted for nanocrystalline semiconductors.[1,5] Tunneling spectroscopy is used to measure the energy gap of Q-InAs and of bulk single-crystal InAs. In TS, the energy gap is obtained from $I-V$ plots by extrapolation of the exponentially increasing current regions to the voltage axis.[33] The (band) gap energy (E_g) then corresponds to this potential region, where tunneling currents should be minimal due to the low density of electronic states. In the case where surface electronic states lie in the energy gap region, a small current may be detected in the corresponding potential range.

$I-V$ plots obtained for unpassivated, bulk p-InAs wafers were unstable in air, and showed features attributed to the presence of surface oxides. Upon treating the surface with sulfide, however, the tunneling spectra stabilized and yielded reproducible E_g measurements, both for replicate spectra acquired at a particular location on the sample surface, as well as for measurements made on different samples. Surface passivation has previously been shown to be mandatory to obtain reliable STM and STS information in air for some compound semiconductors, including GaAs.[34−36] Surface oxides grow on the unpassivated surface upon exposure to air, creating an electrically heterogeneous surface with a large density of surface states within the gap region.[33] Sulfide treatment prevents oxide growth on InAs and other III−V semiconductors, causing a decrease in the density of surface states, yielding a more homogeneous and stable surface.[37] Although sulfide-treated semiconductor surfaces may exhibit a slow degradation in electronic properties with time,[37c] the passivated surfaces are protected against oxidation for several hours, which is sufficient for the purpose of our experiments.

Figure 6a shows a TS $I-V$ plot for a passivated, bulk p-InAs single crystal obtained at a fixed tip−sample

(31) Wang, Y.; Herron, N. *J. Phys. Chem.* **1991**, *95*, 525.
(32) *Semiconductors: Group IV Elements and III−V Compounds*; Madelung, O., Ed.; Springer-Verlag: New York, 1991; pp 134 and 139.
(33) (a) Albrektsen, O.; Arent, D.; Meier, H. P.; Salemink, H. *Appl. Phys. Lett.* **1990**, *57*, 31. (b) Whitman, L. J.; Stroscio, J. A.; Dragoset, R. A.; Celotta, R. J. *Phys. Rev. Lett.* **1991**, *66*, 1338. (c) Whitman, L. J.; Stroscio, J. A.; Dragoset, R. A.; Celotta, R. J. *Phys. Rev. B* **1991**, *44*, 5951.
(34) Silver, R. M.; Dagata, J. A.; Tseng, W. *J. Appl. Phys.* **1994**, *9*, 5122.
(35) Dagata, J. A.; Tseng, W.; Bennett, J.; Schneir, J.; Harary, H. H. *Appl. Phys. Lett.* **1991**, *59*, 3288.
(36) Dagata, J. A.; Tseng, W.; Silver, R. M. *J. Vac. Sci. Technol.* **1993**, *A11*, 1070.
(37) See, e.g.: (a) Iyer, R.; Lile, D. L. *Appl. Phys. Lett.* **1991**, *59*, 437. (b) Oigawa, H.; Fan, J.-F.; Nannichi, Y.; Sugahara, H.; Oshima, M. *Jpn. J. Appl. Phys.* **1991**, *30*, L322. (c) Lu, H. Z.; Graham, M. J.; Feng, X. H.; Yang, B. X. *Appl. Phys. Lett.* **1992**, *60*, 2773. (d) Kuruvilla, B. A.; Ghaisas, S. V.; Datta, A.; Banerjee, S.; Kulkarni, S. K. *J. Appl. Phys.* **1993**, *73*, 4384.

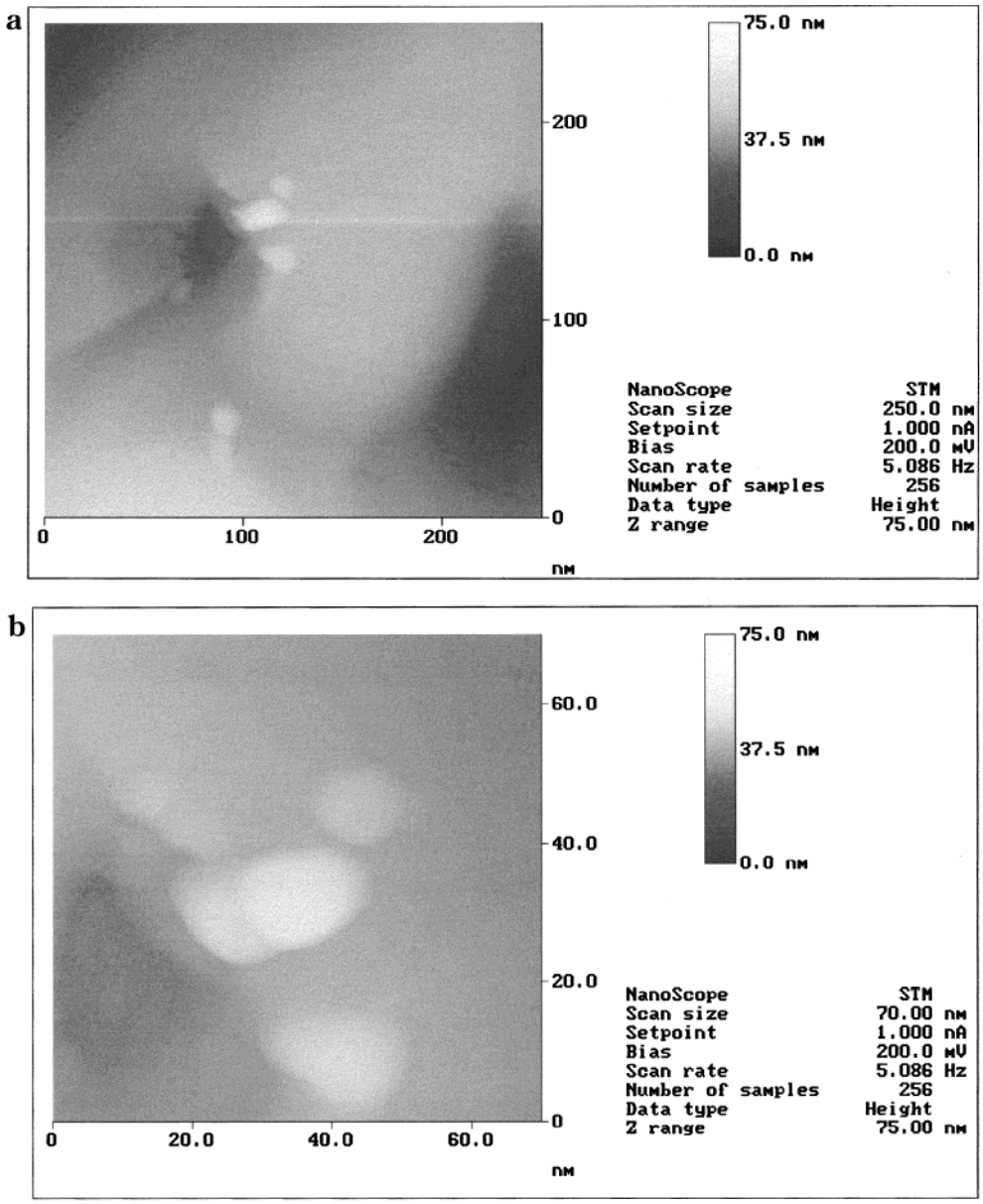

Figure 5. Constant-current mode STM images of single Q-InAs particles on Au/mica surface acquired with a Pt/Ir tip at a 200 mV bias voltage and 1.0 nA current. Panel a represents a 250 nm scan size while panel b is a 70 nm region from that image.

separation distance determined by a 100 mV bias voltage and a set-point current of 1.0 nA, using a relatively blunt Pt/Ir tip to help stabilize the plots.[11] The differential conductance (dI/dV) plot[9−11,13,38] (Figure 6b) shows a conductance gap equal in magnitude to the band gap estimated from Figure 6a. Table 1 shows mean and standard deviation values of E_g measurements obtained from $I-V$ plots. A different location on a single-crystal wafer was examined in each of the three sets of data (each data set was obtained without deliberately translating the tip). In one experiment, the $I-V$ plots were stable over 5 h, during which time the sulfide-treated single crystal p-InAs was exposed to the atmosphere. In this particular set, a mean E_g value of 0.41 ± 0.08 eV was obtained from 38 spectra, in agreement with the accepted value for bulk InAs (0.36 eV at 300 K).

By contrast, sulfide treatment was not effective in protecting the Q-InAs surface against oxidation. $I-V$ plots obtained in air for sulfide-treated Q-InAs on Pt were unstable, yielded a large range in E_g values, and showed the same features attributed to surface oxides on bulk samples. In one set of 15 spectra acquired using a 50 mV initial bias voltage and 1.0 nA set-point current, E_g ranged from 0.241 to 1.90 eV, with a mean value of 0.98 ± 0.44 eV. Since >1% of the constituent atoms can be situated at the interface of a nanoparticle (e.g., ∼2.6% for a 10 nm diameter InAs cluster), protecting the surface against oxidation presents a major concern in the use of TS to study Q-semiconductors.

An alternative approach was undertaken in which TS of Q-InAs/Au under different nonconductive fluids was performed (e.g., methanol, glymes, silicone oil) to decrease exposure of the Q-particles to air. A useful fluid must be nonconductive, and should not strongly interact with the particles to result in desorption. The glymes were found to cause desorption of the particles from the

(38) Zhao, X. K.; McCormick, L.; Fendler, J. H. *Chem. Mater.* **1991**, *3*, 922.

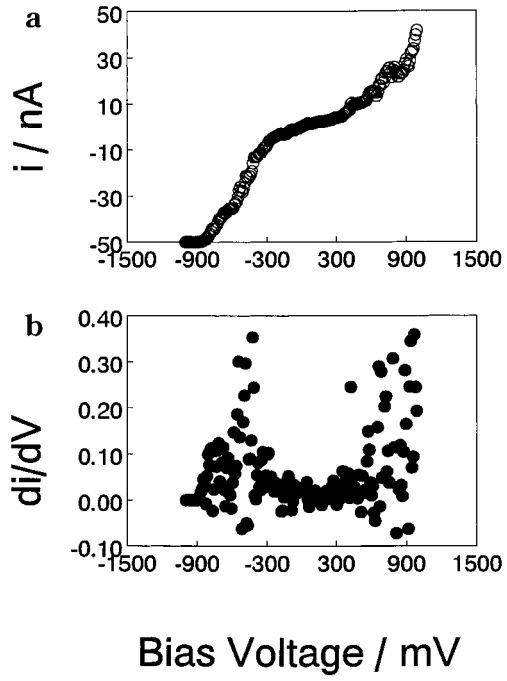

Figure 6. Tunneling $I-V$ plot of p-InAs passivated with a sulfide layer, obtained with a blunt Pt/Ir tip at a bias voltage of 100.1 mV and 1.0 nA set-point current: original $I-V$ curve (a), and differential conductance (dI/dV) format (b).

Table 1. Band Gap Measurements (E_g) Obtained from $I-V$ Plots Acquired at 100 mV Initial Bias Voltage and 1.0 nA Set-Point Current for *p*-InAs Passivated with Sulfide Using a Blunt Pt/Ir Tip

no. of spectra	mean E_g (eV)	SD (eV)
21	0.41	0.05
11	0.34	0.08
38	0.41	0.08

Au substrate (caused by their strong chelating properties toward group III metals), and methanol evaporated too quickly. Silicone oil, on the other hand, did not disrupt the contact with the underlying Au surface. In addition, $I-V$ plots of sulfide passivated, single crystal p-InAs were acquired under this fluid and gave identical band gap values to those samples examined in air. Figure 7a shows a typical tunneling spectrum for Q-InAs/Au examined under silicone oil with a sharp Pt/Ir tip. The TS $I-V$ plot for bare Au (not shown) revealed ohmic behavior, characteristic of clean metallic surfaces.[39] The $I-V$ (Figure 7a) and dI/d$V-V$ (Figure 7b) tunneling plots for Q-InAs films revealed a significantly wider apparent energy gap compared to the bulk material. Data from additional experiments are listed in Table 2, showing gap energy determinations for different locations on a single Q-InAs film and for different Q-InAs films. The energy gap thus measured was on the average of 0.8−1.0 eV; more than twice larger than the band gap of the bulk material. Small variations in the initial bias voltage and set-point current used to set the tip−sample separation distance did not affect E_g determination within the precision of our measurements. One should note here that STM imaging of Q-InAs particles at low bias of 100−200 mV and 1.0 nA current is possible even though the particles have an energy gap of ∼1.0 eV. In the STM experiments, a current of 1.0 nA can be maintained at low bias voltage through states in the energy-gap region of the QDs.

(39) Schott, J. H.; White, H. S. *J. Phys. Chem.* **1994**, *98*, 297.

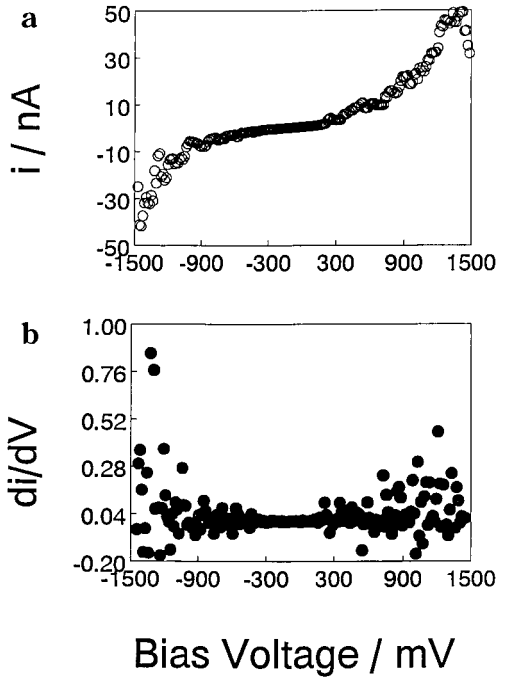

Figure 7. Tunneling $I-V$ plot obtained under silicone oil using a sharp Pt/Ir tip for Q-InAs/Au using a 199.9 mV set-point bias voltage and 1.5 nA set-point current: original $I-V$ curve (a) and differential conductance (dI/dV) format (b).

Table 2. HOMO−LUMO Gap Measurements (E_g) Obtained from $I-V$ Plots of Q-InAs/Au under Silicone Oil Using a Sharp Pt/Ir Tip

no. of spectra	mean E_g (eV)	SD (eV)
21[a]	0.84	0.13
6[b,1]	0.85	0.13
17[b,2]	0.97	0.24

[a] Acquired at 400 mV initial bias voltage and 1.5 nA set-point current [b] Acquired at 200 mV initial bias voltage and 1.5 nA set-point current. *a* and *b* represent different films while *b*,1 and *b*,2 are different locations on the same film.

The larger range of gap energies suggested by the large SDs (Table 2) for the Q-InAs samples compared to bulk InAs may be explained by the presence of a size distribution for Q-InAs which, because of quantum size effects, will lead to a variation in the energy gap. Even when the tip is assumed stationary, different spectra may correspond to neighboring QDs, as a result of mechanical and thermal drifts.

Correlation of Measured Band Gap with Particle Size. Figure 8 is a plot of the energy gap of Q-InAs clusters as a function of the cluster diameter based on effective mass model (EMM)[5] calculations, in which the energy gap of the quantum-confined semiconductor (E) is given by

$$E = E_g + \frac{\hbar^2\pi^2}{2R^2}\left(\frac{1}{m_e{}^* m_e} + \frac{1}{m_h{}^* m_e}\right) - \frac{1.8e^2}{4\pi\epsilon_r\epsilon_o R}$$

where E_g corresponds to the bulk band gap, and R is the particle radius. (The remaining variables and constants have the same definition as above).

By using the above model, the calculated particle sizes corresponding to the measured Q-InAs energy gap (Table 2) ranged between 10 and 12 nm. For example,

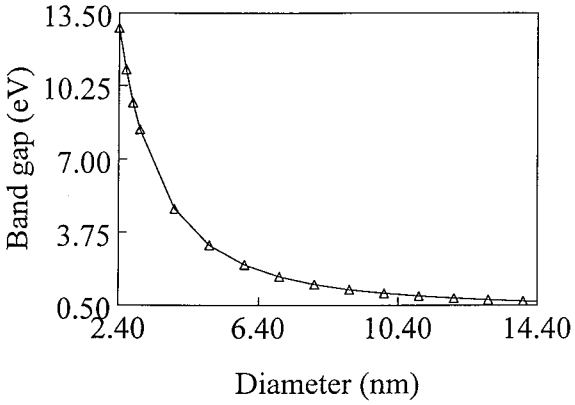

Figure 8. Variation of the energy gap with particle diameter based on EMM calculations.

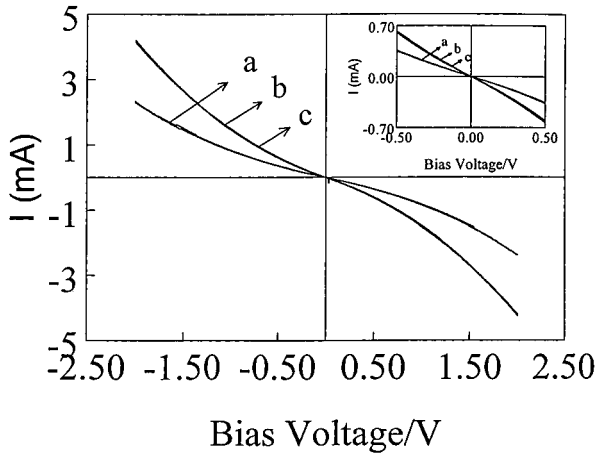

Figure 9. CV acquired under vacuum at 100 mV/s for Q-InAs films deposited on Au IDA electrode. This film was formed by solvent casting of (a) 100, (b) 200, and (c) 300 μL of a 2.5 mg/mL Q-InAs/methanol suspension.

an average energy gap of 0.837 ± 0.126 eV (set of 21 spectra) corresponds to a diameter of 12 ± 2 nm. This size falls within one SD unit of the STM-measured particle size (viz.,11 ± 4 and/or 18 ± 6 nm), and is consistent with XRD and TEM size measurements for these QDs. An analysis of quantum confinement by Kayanuma showed the EMM to be valid only in cases of strong confinement (of the electron and hole), where the ratio of the QD radius (R) to the Bohr radius (a_B) is smaller than 2.[40] For radii larger than the exciton radius, where the ratio R/a_B is larger than 4, weak confinement of the exciton center of mass takes place, and a variational method was employed to predict the extent of confinement.[40] Furthermore, it is found that the EMM fails for very small semiconductor clusters, yielding an overestimation of quantum confinement, because the assumption of parabolic bands fails in this region.[31,41,42] For very small clusters, a tight binding calculation was shown by Lippens and Lannoo to yield a better prediction of quantum confinement.[42] In the case of the Q-InAs clusters examined in this work, the ratios R/a_B (viz., using R = 5.5 and 9 nm from the constant-height and constant-current modes, respectively), are calculated to be 0.17 and 0.29. Therefore, according to the above analysis, the Q-InAs particles are expected to exhibit strong quantum confinement effects, correctly predicted by the EMM.

Next, we discuss possible contributions to the TS data from charge transport between the Q-InAs nanoparticles and at the Q-InAs/Au interface; "band bending" in the quantum dots; and Coulomb blockade effects. We conclude that the TS-measured increase in the energy gap of Q-InAs relative to the bulk solid is most likely caused by quantum size effects in the sample. Although our results are the first with respect to III−V materials, TS has been used for probing quantum confinement effects in Q-particles, with studies on CdS[13,43] and CdSe[14] having already been published.

Conductivity Measurements of Q-InAs Films on Au IDAs. In TS studies of multilayered films of QD semiconductors deposited on metal surfaces, the effect of charge transport at the particle/particle, and the metal/particle interfaces on the TS data must be considered. One concern is that charge conduction across a barrier height at interfaces (*hypothetically*, by analogy to a Schottky barrier at metal-bulk semiconductor and to a bulk semiconductor−semiconductor interface) could contribute to the zero-current region of the TS spectra, and affect energy-gap measurements.

Charge transport between Q-InAs and Au, and between the Q-InAs particles themselves was studied by acquiring (macroscopic) $I-V$ plots of Q-InAs films on Au IDA electrodes. Figure 9 shows typical $I-V$ behavior of such films, deposited by casting 100 (a), 200 (b), and 300 (c) μL of a Q-InAs/methanol suspension on Au IDA electrodes. These plots were acquired under vacuum, by scanning the potential between −2.0 and +2.0 V at 100 mV/s, and were virtually identical on the forward and reverse sweeps of each CV, thus sweeping the potential did not alter the films' electrical characteristics. The $I-V$ plots showed linear behavior at low potential, revealing no potential region of zero conduction, which could contribute to the low-current region in the TS of Q-InAs films on Au, in a similar way to the effect of a Schottky contact to a bulk semiconductor on tunneling data. Because of the similarity of these quantum dots to molecules, the picture is fundamentally different from solid-state behavior, as further discussed below, and charge transport can take place via a quite different (hopping) mechanism at interfaces.

$I-V$ plots of Q-InAs films under vacuum were identical for different films formed using the same volumes, and for the same film during a period of several days. By contrast, $I-V$ plots measured under ambient conditions or under argon were not reproducible. This behavior was attributed to Q-InAs oxidation in air, as well as adsorption of solvent vapors in the argon-filled chamber, which could alter the films' conductivity. Film conductivities were calculated from the linear region[44] of the $I-V$ plots between +0.5 and −0.5V. The determining distance for conductivity calculations is the 5

(40) Kayanuma, Y. *Phys. Rev. B.* **1988**, *38*, 9797.
(41) See e.g.: (a) Wang, Y.; Suna, A.; Mahler, W.; Kasowski, R. *J. Chem. Phys.* **1987**, *87*, 7315. (b) Miyoshi, H.; Yamashima, M.; Yoneyama, H. *J. Chem. Soc., Faraday Trans.* **1990**, *86*, 815.
(42) (a) Lippens, P. E.; Lanoo, M. *Phys. Chem. B.* **1989**, *39*, 10935. (b) Lippens, P. E.; Lanoo, M. *Mater. Sci. Eng. B* **1991**, *9*, 485.
(43) Miyake, M.; Matsumoto, H.; Nishizawa, M.; Sakata, T.; Mori, H.; Kuwabata, S.; Yoneyama, H. *Langmuir* **1997**, *13*, 742.
(44) Terrill, R. H.; Postlethwaite, T. A.; Chen, C.; Poon, C.; Terzis, A.; Chen, A.; Hutchison, J. E.; Clark, M. R.; Wignall, G.; Londono, J. D.; Superfine, R.; Falvo, M.; Johnson, C. S., Jr.; Samulski, E. T.; Murray, R. W. *J. Am. Chem. Soc.* **1995**, *117*, 12537.

μm separation distance between two adjacent but opposing Au fingers of the IDA. Q-InAs films formed by evaporating 200−350 μL of a Q-InAs/methanol suspension ("thick films") showed the same $I-V$ behavior under vacuum (cf. parts b and c of Figure 9), while "thinner" films formed by casting 100 μL exhibited lower conductivities (cf. Figure 9a). The shapes of the $I-V$ plots were however similar for all the thicknesses examined. The mean conductivity of the thick films was found to be $(2.1 \pm 0.2) \times 10^2\ \Omega^{-1}\ m^{-1}$ (14 measurements from different films), while thinner films exhibited an average conductivity of $(1.2 \pm 0.2) \times 10^2\ \Omega^{-1}\ m^{-1}$ (4 measurements). The larger resistivities of thinner films could have resulted from insufficient coverage of the underlying insulating substrate. The conductivity of the Q-InAs thick films ($2.1 \times 10^2\ \Omega^{-1}\ m^{-1}$) was only 2 orders of magnitude lower than the conductivity of bulk single-crystal InAs ($10^4\ \Omega^{-1}\ m^{-1}$).[45] This is higher than expected for an intrinsic bulk semiconductor of the same band gap as these QDs. Although the number of investigations of Q-semiconductors has been growing rapidly,[46] these have not been characterized in terms of their conductivities. The conductivity of a bulk semiconductor depends on the magnitude of its band gap, on the dopant concentration, and the charge mobility. On the other hand, what dictates charge conduction through these Q-semiconductors can be different from the bulk material because of their hybrid state between molecular and solid-state behavior. One should also note that because of the dots' small dimensions, a single or a few impurity atoms can constitute a significant perturbation to the dots as to have a considerable effect on their electrical properties.

Other Possible Influences on TS Results for Q-InAs. InAs is different from most III−V semiconductors in that the Fermi level of common metals is pinned above its conduction band (CB) edge.[47] As a consequence of this, in addition to its relatively narrow band gap (0.36 eV), and its large electron and hole mobilities (33 000 and 460 $cm^2\ V^{-1}\ s^{-1}$, respectively),[48] InAs forms low resistance contacts to metals.[48−53] The interaction between Q-InAs and metals (viz., the STM tip or the underlying metal) is, however, fundamentally different from that of bulk InAs, because of the absence of a band structure in the QDs and their similarity to molecules, albeit very large; in addition to their wider HOMO−LUMO separation.

When a voltage drop occurs inside a semiconductor with a band structure, band bending takes place and a space charge region forms. The width of the resulting space charge region, W, associated with a typical metal−semiconductor junction or a metal−insulator−semiconductor junction is given by[54]

$$W = \left[\frac{(2\epsilon_o\epsilon_r)eV}{e^2\ N_d}\right]^{1/2}$$

where eV is the difference in energy between an electron at the surface of the semiconductor and an electron in the bulk (equivalent to the extent of band bending), N_d is the charge carrier density, ϵ_o is the permittivity of free space, and ϵ_r is the dielectric constant of the semiconductor.

For very small tip-semiconductor separation distances, tip-induced band bending may occur at zero applied bias.[43,55] Band bending can also occur upon contact of a semiconductor with an underlying metal, and can have a contribution from the applied bias voltage between the tip and the semiconductor sample.[54] In these cases, band bending will have a considerable effect on the shape of the TS plots and the magnitude of the energy gap measured. The picture is quite different for a cluster because of its confined dimensions. For example, when $V = 0.5$ V, and $N_d = 10^{22}\ m^{-3}$, W is calculated to be 250 nm, which is larger than a 10 nm Q-InAs cluster. To further illustrate this point, *hypothetically*, W would become equal to a cluster diameter of 10 nm for a band bending $eV = 0.8$ neV when $N_d = 10^{16}\ m^{-3}$, or 0.8 meV when $N_d = 10^{22}\ m^{-3}$. Clearly, "band bending" similar to bulk semiconductors cannot occur to any appreciable extent in a QD of the size studied here. Experimentally, the absence of tip-induced "band bending" was evident in the independence of the tunneling spectra of variation in the tip−sample separation distance (see Table 2).

We also argue that single electron tunneling known as Coulomb blockade effect[56] is less likely to have contributed to the observed increase in the zero-current region in the TS spectra of 10−20 nm size Q-InAs. Single-electron tunneling occurs when the charging energy ($E_c = e^2/2C$; where C is the capacitance) is considerably larger than the thermal energy (k_BT), usually for small clusters at low temperatures. In this case, tunneling of electrons occurs one at a time when a voltage equal to the Coulomb barrier is applied; resulting in the observation of peaks in the conductance plots.[57] Most of the experimental work reported on Coulomb blockade has been done on mesoscopic structures at very low temperatures.[56b,58] Because the charg-

(45) Van Vlack, L. H. In *Elements of Materials Science and Engineering*; Addison-Wesley Publishing Company, Inc.: Reading, MA, 1985; Chapter 8, p 306.
(46) See, e.g.: (a) Fischer, C.-H.; Henglein, A. *J. Phys. Chem.* **1989**, *93*, 5578. (b) Colvin, V. L.; Goldstein, A. N.; Alivisatos, A. P. *J. Am. Chem. Soc.* **1992**, *114*, 5221. (c) Hobson, R. A.; Mulvaney, P.; Grieser, F. J. *Chem. Soc., Chem. Commun.* **1994**, 823. (d) Zorman, B.; Ramakrishna, M. V.; Freisner, R. A. *J. Phys. Chem.* **1995**, *99*, 7649. (e) Noglik, H.; Pietro, W. J. *Chem. Mater.* **1995**, *7*, 1333.
(47) Mead, C. A.; Spitzer, G. W. *Phys. Rev.* **1964**, *134*, A713.
(48) Katz, A.; Chu, N. G.; Weir, B. E.; Dautremont-Smith, W. C.; Logan, R. A.; Tabun-Ek, T. *J. Appl. Phys.* **1990**, *68*, 4141.
(49) Woodall, J. M.; Freeouf, J. L.; Pettit, G. D.; Jackson, T.; Kirchner, P. *J. Vac. Sci. Technol.* **1981**, *19*, 626.
(50) Peng, C. K.; Chen, J.; Chyi, J.; Morkoç, H. *J. Appl. Phys.* **1988**, *64*, 429.
(51) Kol'tsov, G. I.; Krutenyuk, Y. V. *Fiz. Tekh. Poluprovodn.* **1989**, *23*, 1986; *Sov. Phys. Semicond.* **1989**, *23*, 1229.
(52) Shen, T.-H.; Elliott, M.; Williams, R. H.; Westwood, D. *Appl. Phys. Lett.* **1991**, *58*, 842.
(53) Stareev, G.; Künzel, H. *J. Appl. Phys.* **1993**, *74*, 7592.
(54) Sapoval, B.; Hermann, C. *Physics of Semiconductors*; Springer-Verlag: New York, 1995; p 234.
(55) Kaiser, W. J.; Bell, L. D.; Hecht, M. H.; Grunthaner, F. J. *J. Vac. Sci. Technol. A* **1988**, *6*, 519.
(56) (a) Tinkham, M. *Am. J. Phys.* **1996**, *64*, 343. (b) Livermore, C.; Crouch, C. H.; Westervelt, R. M.; Campman, K. L.; Gossard, A. C. *Science* **1996**, *274*, 1332.
(57) (a) Smith, T. P., III; Lee, K. Y.; Knoedler, C. M.; Hong, J. M.; Kern, D. P. *Phys. Rev. B* **1988**, *38*, 2172. (b) Johnson, A. T.; Kouwenhoven, L. P.; de Jong, W.; van der Vaart, N. C.; Harmans, C. J. P. M.; Foxon, C. T. *Phys. Rev. Lett.* **1992**, *69*, 1592.
(58) (a) Guéret, P.; Blanc, N.; Germann, R.; Rothuizen, H. *Phys. Rev. Lett.* **1992**, *68*, 1896. (b) Foxman, E. B.; McEuen, P. L.; Meirav, U.; Wingreen, N. S.; Meir, Y.; Belk, P. A.; Wind, S. J. *Phys. Rev. B.* **1993**, *47*, 10020.

ing energy increases with decreasing cluster size (due to a decrease in the capacitance), TS spectra of ultrasmall clusters can be expected to exhibit stepwise tunneling at higher temperatures. At room temperature (RT), this effect has been observed in TS studies of ultrasmall Au islands $\sim 4 \pm 0.5$ nm in size,[59] and Q-CdSe of $\sim$4 nm diameter.[14] On the other hand, TS report of $\sim$4 nm Q-CdS deposited as a monolayer on Au did *not* show evidence of Coulomb blockade at RT.[13] No reports exist about RT single electron tunneling in larger crystallites. On the basis of the existing experimental work on Coulomb blockade, there is no evidence yet to believe that charging effects have resulted in a Coulomb gap and contributed to the RT tunneling data of the 10−20 nm Q-InAs clusters studied in this work.

Conclusions

STM images of films and of single Q-InAs particles deposited on Au and Pt surfaces revealed dimensions well below the estimated exciton diameter for InAs, in agreement with XRD and TEM size measurements. TS $I-V$ plots of Q-InAs films on Au were compared to TS $I-V$ plots for single-crystal InAs, passivated with a sulfide layer, and revealed a larger zero-current region for Q-InAs relative to the bulk solid, believed to be due to quantum confinement effects in the nanoparticles. $I-V$ measurements under vacuum of Q-InAs films on Au IDAs indicated the absence of an effect of a barrier-height to charge conduction at interfaces on the tunneling $I-V$ plots. These $I-V$ measurements also revealed Q-InAs film conductivities only 2 orders of magnitude lower than bulk single-crystal InAs; such a large conductivity can be attributed to the molecular-like properties of these clusters.

Acknowledgment. This work was supported in part by the Air Force Office of Scientific Research (F-49620-93-1-0004). We thank Dr. Shreyas Kher and Dr. Michael S. Lube (Duke University, Department of Chemistry) for synthesizing the Q-particle sample, Kausar Banoo (Duke University, Electrical Engineering) for assistance in preparing ohmic contacts to single crystal electrodes, and Professor Hisham Massoud (Duke University, Electrical Engineering) for access to the clean room facility. We also thank Rob Willicut and Professor Robin McCarley (Louisiana State University, Department of Chemistry) for preparing the Au/mica substrates.

CM9902927

(59) Schönenberger, C.; van Houten, H.; Donkersloot, H. S. *Europhys. Lett.* **1992**, *20*, 249.